

The University of Bradford Institutional Repository

<http://bradscholars.brad.ac.uk>

This work is made available online in accordance with publisher policies. Please refer to the repository record for this item and our Policy Document available from the repository home page for further information.

To see the final version of this work please visit the publisher's website. Available access to the published online version may require a subscription.

Link to original published version: <http://dx.doi.org/10.14359/19855>

Citation: Yang, K.H. and Ashour, A.F. (2008) Effectiveness of Web Reinforcement around Openings in Continuous Concrete Deep Beams. ACI Structural Journal, Vol. 105, No. 4, pp. 414-424.

Copyright statement: © 2008 ACI. Reproduced in accordance with the publisher's self-archiving policy.



EFFECTIVENESS OF WEB REINFORCEMENT AROUND OPENINGS IN CONTINUOUS CONCRETE DEEP BEAMS

K. H. Yang^a and A. F. Ashour^b

^a *Corresponding author, Department of Architectural Engineering, Mokpo National University, Mokpo, Jeonnam, South Korea*

^b *EDT1, School of Engineering, Design and Technology, University of Bradford, Bradford, BD7 1DP, UK.*

Biography: **K. H. Yang** is currently a visiting research fellow at the University of Bradford, UK and an assistant professor at Mokpo National University, Korea. He received his MSc and PhD degrees from Chungang University, Korea. His research interests include ductility, strengthening and shear of reinforced high-strength concrete structures.

A.F.Ashour is a senior lecturer at the University of Bradford, UK. He obtained his BSc and MSc degrees from Mansoura University, Egypt and his PhD from Cambridge University, UK. His research interests include shear, plasticity and optimisation of reinforced concrete and masonry structures.

ABSTRACT

Twenty two reinforced concrete continuous deep beams with openings and two companion solid deep beams were tested to failure. The main variables investigated were the configuration of web reinforcement around openings, location of openings, and shear span-to-overall depth ratio. The influence of web reinforcement on controlling diagonal crack width and load capacity of continuous

deep beams with openings was significantly dependent on the location of openings. The development of diagonal crack width and load capacity of beams having openings within exterior shear spans were insensitive to the configuration of web reinforcement. However, for beams having openings within interior shear spans, inclined web reinforcement was the most effective type for controlling diagonal crack width and increasing load capacity. It has also observed that higher load and shear capacities were exhibited by beams with web reinforcement above and below openings than those with web reinforcement only above openings. The shear capacity at failed shear span of continuous beams tested is overestimated using Kong et al's formula developed for simple deep beams with openings.

Keywords: continuous deep beams, openings, web reinforcement, load capacity, shear capacity.

INTRODUCTION

Openings are frequently provided in reinforced concrete deep beams to facilitate essential services, such as ventilating ducts, water supply and drainage pipes, network access or even movement from one room to another. However, most experimental¹⁻⁴ and theoretical⁵⁻⁷ investigations to evaluate the shear strength of such members focused on simply supported deep beams with openings. There are very few, if any, tests of continuous deep beams with different web reinforcement arrangement around web openings. Furthermore, their design details have not been yet provided by most code provisions⁸⁻¹¹, though web openings have a significant effect on the shear capacity and load transfer mechanism of deep beams.

Kong et al.⁵ tested eight simply supported deep beams reinforced with various arrangements of web reinforcement around openings and concluded that the inclined web reinforcement was the most effective form for controlling diagonal crack width and increasing the shear capacity. Tan et al.⁶ also pointed out that web reinforcement in the lower load path below openings was not effective based

on a theoretical analysis of simply supported deep beams using strut-and-tie model. However, the influence of web reinforcement around openings on the load capacity of continuous deep beams would be dissimilar to that of simple deep beams. Experimental studies¹²⁻¹⁴ showed that the failure mechanism and load capacity of continuous deep beams are different from those of simple deep beams owing to the coexistence of high shear and high moment in interior shear spans and the development of tensile strains in both longitudinal top and bottom reinforcements. This would cause a significant reduction in the effective strength of concrete struts that are the main load transfer element in deep beams.

The main objective of this study is to assess the effect of web reinforcement around openings on diagonal crack width and load capacity of continuous deep beams. Twenty-two two-span reinforced concrete deep beams with web openings and two companion solid deep beams were tested to failure. The main variables investigated were the configuration of web reinforcement around openings, location of openings, and shear span-to-overall depth ratio. The shear capacity of beams tested is compared with Kong et al.'s empirical formula calibrated against test results of simple deep beams with web openings.

TEST SPECIMENS

Geometrical dimensions and opening size

Table 1 and Fig. 1 show the geometrical dimensions and web reinforcement arrangement around openings of test specimens. All beams tested had the same section width b_w of 160 mm and overall depth h of 600 mm. The shear span-to-overall depth ratios a/h , where a = the shear span, were selected to be 0.6 and 1.0. Web openings were located in either interior or exterior shear spans as shown in Fig. 2. The opening size was selected as $0.5a \times 0.2h$ to produce an opening area ratio ρ_{OA} , which is the ratio of the opening area to shear span area, of 0.1 regardless of variation of the shear

span-to-overall depth ratio. The width and depth of openings were 180 mm and 120 mm, respectively, for beams having $a/h=0.6$, and 360 mm and 120 mm, respectively, for beams having $a/h=1.0$. In each beam tested, the opening centre was positioned in accordance with that of the shear span area to completely interrupt the natural load path joining the edges of load and support plates as shown in Fig. 1.

Steel reinforcement

The configuration of web reinforcement around openings included four different arrangements as shown in Fig. 1: none, only vertical, only horizontal, and only inclined reinforcement. To assess the effectiveness of web reinforcement below openings, the arrangement of web reinforcement was classified into two groups, one of which was U-type for web reinforcement only placed above openings as shown in Fig. 1 (b) to Fig. 1 (d), and the other was B-type for web reinforcement symmetrically placed at both above and below openings as given in Fig. 1 (e) to Fig. 1 (g). Beams having openings within exterior shear spans had only U-type web reinforcement, while beams having openings within interior shear spans had either U-type or B-type web reinforcement.

For all beams tested, the longitudinal top, $\rho_s' \left(= \frac{A_s'}{b_w d} \right)$, and bottom, $\rho_s \left(= \frac{A_s}{b_w d} \right)$, reinforcement ratio were kept constant at 1%, where A_s' and A_s are the area of longitudinal top and bottom reinforcement, respectively, and d is the section effective depth. The clear cover to the longitudinal top and bottom reinforcement was 35 mm. The longitudinal bottom reinforcement was continuous over the full length of the beam and welded to 160×100×10 mm end plates, whereas the longitudinal top reinforcement was anchored outside exterior supports by 90° hook according to ACI 318-05. Three deformed steel bars of 10 mm diameter were vertically, horizontally or diagonally arranged as web reinforcement around openings. The vertical web reinforcement was closed stirrups and evenly placed along the opening width as shown in Fig. 1 (b) and Fig. 1 (e). The

horizontal web reinforcement with 90° hook was arranged along the depth of top chord above openings or bottom chord below openings as shown in Fig. 1 (c) and Fig. 1 (f). The angle of all inclined reinforcement was chosen to be 45° to the longitudinal axis of beams tested as shown in Fig. 1 (d) or Fig. 1 (g). Both horizontal and inclined web reinforcements were placed at a spacing of 30 mm at both sides of the beams and satisfied the development length specified in ACI 318-05. In all beams with openings, two horizontal deformed steel bars of 10 mm diameter were placed immediately above openings to ease the arrangement of vertical web reinforcement and transfer tensile forces by strut-and-tie action as suggested by Tan et al.⁶

Beam notation

The beam notation given in Table 1 includes four parts except for the companion solid deep beams, 6N and 10N. The first part is used to identify the shear span-to-overall depth ratio: 6 for $a/h=0.6$ and 10 for $a/h=1.0$. The second part refers to the opening location: E for web openings within exterior shear spans and I for web openings within interior shear spans. The third part gives configuration of web reinforcement: N for no web reinforcement, V for vertical web reinforcement, H for horizontal web reinforcement, and I for inclined web reinforcement. The last part explains the type of web reinforcement: N for no web reinforcement, U for U-type web reinforcement, and B for B-type web reinforcement. For example, the notation 6EVU identifies a continuous deep beam with web openings within exterior shear spans, having shear span-to-overall depth ratio of 0.6 and vertical web reinforcement of U-type.

Material properties

The ingredients of ready-mixed concrete used to cast the test specimens were ordinary portland cement, fly-ash, irregular gravel of a maximum size of 25 mm, and sand. Design concrete strength was 55 MPa. Control cylinders were cast and cured simultaneously with beams to determine the

compressive strength of concrete. The compressive strength of concrete obtained from testing three cylinders is given in Table 1.

Both longitudinal top and bottom reinforcement consisted of three steel bars of 19 mm diameter, 560 MPa yield strength and 200 GPa elastic modulus. The web reinforcement around openings was normal mild steel bars having yield strength of 420 MPa and elastic modulus of 195 GPa.

Test set-up

Fig. 2 shows the loading and instrumentation arrangement of beams tested. All beams having two spans were tested to failure under a symmetrical two-point top loading system with a loading rate of 30 kN/min using a 3000 kN load capacity universal testing machine (UTM). Each span was identified as E-Span or W-span as shown in Fig. 1 and Fig. 2. The two exterior end supports are designed to allow horizontal and rotational movements, whereas the intermediate support prevents horizontal movement but allows rotation. In order to evaluate the shear force and loading distribution, 1000 kN capacity load cells were installed in both exterior end supports. At the location of loading or support point, a steel plate of 100 mm, 150 mm or 200 mm wide was provided to prevent premature crushing or bearing failure as shown in Fig. 2.

Vertical deflections at mid-spans and support settlements were measured using linear variable differential transformers (LVDTs). The PI type gages were used for measuring diagonal crack width at concrete struts as shown in Fig. 2. Strains in web reinforcement were recorded by 5 mm electrical resistance strain gages (ERS) located at different positions as shown in Fig. 1. The test data were captured by a data logger and automatically stored.

TEST RESULTS AND DISCUSSION

Crack propagation and failure modes

The crack propagation and failure mode of continuous deep beams with web openings were strongly influenced by the location of openings and shear span-to-overall depth ratio but independent on web reinforcement around openings as observed in Ashour and Rishi's tests¹⁵. Typical crack propagation and failure modes of beams tested are given in Fig. 3 according to the shear span-to-overall depth ratio and location of openings. A symmetrical crack pattern was observed for both E and W spans of the deep beams tested before failure. The first crack in all beams tested except solid beams occurred at opening corners near load points (at B and D in Fig. 2) and propagated toward load points, and then diagonal cracks at opening corners opposite to load points (at A and C in Fig. 2) appeared with the load increase as given in Table 2. For beams having web openings within exterior shear spans, flexure cracks in hogging and sagging zones occurred almost simultaneously with a diagonal crack within the interior shear span after the occurrence of diagonal cracks around openings. For beams having web openings within interior shear spans, most cracks concentrated in the corners of openings and diagonal cracks at exterior shear spans didn't appear in most beams having $a/h=1.0$ as given in Table 2. The failure mode of the beams tested can be categorised into two modes according to the location of openings as shown in Fig. 3 and given in Table 2: mode A for beams having failure planes along diagonal concrete struts at interior shear spans (see Fig. 3 (b) and Fig. 3 (d)), and mode B for beams having failure planes at both interior and exterior shear spans (see Fig. 3 (a) and Fig. 3 (c)). All beams having openings within interior shear spans failed in mode A, which had failure planes formed along the upper load path joining the edge of load plate and opening corner opposite to the load point (at A in Fig. 2 (b)) and lower load path connecting the edge of intermediate support plate and opening corner opposite to the intermediate support (at C in Fig. 2 (b)). The companion solid deep beams had a similar failure to mode A, where failure planes formed

along the natural load path joining the edges of load and intermediate support plates. On the other hand, all beams having openings within exterior shear spans failed in mode B.

Load versus mid-span deflection

Mid-span deflections at failed span for different beams tested having $a/h=0.6$ against the total applied load are shown in Fig. 4: Fig. 4 (a) for beams having openings within exterior shear spans, Fig. 4 (b) for beams having openings within interior shear spans and U-type web reinforcement, and Fig. 4 (c) for beams having openings within interior shear spans and B-type web reinforcement. The influence of web reinforcement around openings on the load-deflection relationship of tested beams having $a/h=1.0$ was similar to that of beams having $a/h=0.6$. The initial stiffness of beams with openings was almost the same as that of the companion solid deep beams, regardless of the configuration of web reinforcement around openings. After the first diagonal crack appeared at the web opening corners, the mid-span deflection of beams sharply increased compared with that of the companion solid deep beams and higher increasing rate of deflection developed in beams having openings within interior shear spans than in beams having openings within exterior shear spans. For beams having openings within exterior shear spans, the increasing rate of deflection was not influenced by the configuration of web reinforcement. On the other hand, the configuration of web reinforcement on the increasing rate of deflection and failure characteristics clearly influenced beams having openings within interior shear spans. Inclined web reinforcement was the most effective type for reducing deflection of beams with openings. In particular, beam 6IIB having inclined web reinforcement above and below openings showed some ductile behavior at failure despite of the compressive splitting failure of concrete struts as shown in Fig. 4 (c).

Support reactions

The location of openings had a significant influence on support reactions as observed in Ashour and Rishi's tests¹⁵. Fig. 5 shows the amount of load transferred to the intermediate and end supports against the total applied load for beams without web reinforcement including the companion solid deep beams: Fig. 5 (a) for beams having $a/h=0.6$, and Fig. 5 (b) for beams having $a/h=1.0$. On the same figure, the support reactions of the companion solid deep beams obtained from a linear two-dimensional finite element (2-D FE) analysis are also presented. It was shown in a companion paper¹⁴ that the maximum differential support settlement was below $L/17000$ for the test set-up shown in Fig. 2. This differential support settlement has a very little effect, if any, on the redistribution of internal stresses and the development of additional moment and shear. For continuous solid deep beams 6N and 10N, the measured support reactions showed good agreement with those predicted by the linear 2-D FE analysis. Whereas, after the occurrence of the first diagonal crack, there was large difference between support reactions of continuous deep beams with web openings and their companion solid deep beams regardless of the shear span-to-overall depth ratio. For example, for beams having web openings within exterior shear spans, the amount of load transferred to end supports decreased and the intermediate support reaction increased relative to those of the companion solid deep beams, whereas reverse distribution was observed for beams with web openings within interior shear spans.

The ratio of the measured end support reaction at failure and that predicted from linear 2-D FE analysis, $(R_E)_{Exp.}/(R_E)_{FE}$, for different web reinforcement configuration is presented in Fig. 6: Fig. 6 (a) for beams having $a/h=0.6$ and Fig. 6 (b) for beams having $a/h=1.0$. The end support reaction increased for beams having web openings within interior shear spans, whereas it reduced for beams having web openings within exterior shear spans, regardless of the shear span-to-overall depth ratio, a/h . The web reinforcement arrangement around web openings had also some effect

on the distribution of support reactions. The inclined B-type web reinforcement was the most effective in producing end support reaction similar to the corresponding solid deep beam.

Diagonal crack width

Fig. 7 shows the development of diagonal crack width in concrete struts of tested beams with web reinforcement and having $a/h=0.6$ against the total load: Fig. 7 (a) for crack width along line AE shown in Fig. 2. (a) in beams having openings within exterior shear spans and U-type web reinforcement, Fig. 7 (b) for crack width along line AE shown in Fig. 2 (b) in beams having openings within interior shear spans and U-type web reinforcement, and Fig. 7 (c) for crack width along line CF shown in Fig. 2 (b) in beams having openings within interior shear spans and B-type web reinforcement. The influence of web reinforcement around openings on controlling diagonal crack width in beams having $a/h=1.0$ was practically similar to that in beams having $a/h=0.6$. For beams having openings within exterior shear spans, the development of diagonal crack width was nearly independent on the configuration of web reinforcement, and none of web reinforcement reached their yield strain at failure as shown in beams 6EVU, 6EHU, and 6EIU of Fig. 8 which presents the strain in web reinforcement against the total applied load. On the other hand, for beams having openings within interior shear spans, inclined web reinforcement was more effective in controlling diagonal crack width than vertical or horizontal web reinforcement. The effect of inclined web reinforcement in controlling diagonal crack width was more prominent in beams with B-type than that in beams with U-type. The strains of inclined and vertical web reinforcement below openings sharply increased with the occurrence of the first diagonal crack, and then reached the yield strain before failure as exhibited by beams 6IVB and 6IIB in Fig. 8.

Ultimate load and shear capacities

The effect of web reinforcement configuration on the normalized ultimate load capacity

$\lambda_n = \frac{P_n}{2b_w h \sqrt{f'_c}}$, and normalized shear capacity $\eta_n = \frac{V_n}{b_w h \sqrt{f'_c}}$ at the failed shear span of test

specimens are shown in Fig. 9 and Fig. 10, respectively, and Table 2. Overall, load and shear capacities reduced with the increase in shear span-to-overall depth ratio. The load capacity of beams having openings within exterior shear spans was 10~15% smaller than that of the companion solid deep beams, but the shear capacity at failed shear spans of such beams dramatically decreased by 40~50% of the companion solid deep beams, irrespective of shear span-to-overall depth ratio. The load and shear capacities of beams having openings within exterior shear spans were insensitive to reinforcement arrangement around openings as failure planes formed within interior shear spans. On the other hand, for beams having openings within interior shear spans, both the load and shear capacities sharply decreased in comparison with the companion solid deep beams.

The web reinforcement around openings had a higher influence on both load and shear capacities of beams having openings within interior shear spans than beams having openings within exterior shear spans. Inclined web reinforcement was the most effective form for increasing load and shear capacities of continuous deep beams with openings, similar to simple deep beams with openings^{4, 5, 7}. In addition, for beams having openings within interior shear spans, the load and shear capacities of beams with B-type web reinforcement were higher than those of the corresponding beams with U-type web reinforcement. This indicates that the web reinforcement below openings has a significant influence on the load and shear capacities of continuous deep beams with openings within interior shear spans, unlike that observed by Tan et al.⁶ for simple deep beams with openings.

Comparison of test results with Kong et al's formula

The few theoretical investigations in the literature⁵⁻⁷ to evaluate the shear strength of deep beams with openings focused on simply supported deep beams. In addition, no code provisions are available for the design of such members. Kong et al.⁵ proposed an idealised load path based on the failure mode observed in simple deep beams with openings and having shear span-to-overall depth ratio less than 0.4, as shown in Fig. 11. When the opening interrupts the natural load path joining the edges of load and support plates, main load path is turned to the lower path connecting the edge of the support plate and opening corner opposite to support. Hence, by modifying the equation of the shear capacity of solid deep beams, the shear capacity of deep beams with openings was proposed as follows⁵:

$$V_n = C_1 \left[1 - 0.35 \frac{k_1 x}{k_2 h} \right] \sqrt{f_c} b_w k_2 h + C_2 \lambda_2 \sum_{i=1}^n \frac{A_i y_i \sin^2 \alpha_i}{h} \quad (1)$$

where $C_1 = 1.40$ for normal-weight concrete and 1.35 for lightweight concrete, $C_2 = 300\text{N/mm}^2$ for deformed bars and 130N/mm^2 for plain round bars, $\lambda_2 =$ empirical coefficient, 1.0 for longitudinal bottom reinforcement and 1.5 for web reinforcement, b_w and $h =$ width and overall depth of beam, respectively, $k_1 x =$ distance between the inside edge of support plate and opening corner C in Fig 11, $k_2 h =$ distance from the soffit of beam to bottom surface of opening, $n =$ number of reinforcement crossing upper and lower load path, $A_i =$ area of reinforcing bar i , $y_i =$ distance between top surface of beam and reinforcing bar i crossing the upper or lower load path, $\alpha_i =$ angle between the reinforcement i and either upper or lower load path. The shear capacity of solid deep beams can be also calculated from Eq. (1) provided that 1.0 is used for coefficients k_1 and k_2 . In Eq. (1), the first term and second term in the right hand side give the contribution of concrete strut below openings and longitudinal and web reinforcement, respectively to the shear capacity. Eq. (1)

shows that the lower the reinforcement is placed, the more effective its contribution to the beam load capacity.

Fig. 12 and Table 2 show the comparison of measured and predicted shear capacities at the failed shear span of beams tested. The mean and standard deviation of the ratio between predicted and experimental shear capacities $(V_n)_{Pro.} / (V_n)_{Exp.}$ of the continuous deep beams with openings are 1.15 and 0.18, respectively. Predictions obtained from Kong et al's formula commonly overestimate the shear capacity of continuous deep beams with openings, and are closer to the experimental results for beams having shear span-to-overall depth ratio of 0.6 than those of shear span-to-overall depth ratio of 1.0 as Eq. (1) is experimentally calibrated against test results of simple deep beams having a shear span-to-overall depth ratio of 0.4.

CONCLUSIONS

To study the influence of web reinforcement around openings on the structural behaviour of reinforced concrete continuous deep beams, twenty four beams including two companion solid deep beams were tested to failure. Based on test results, the following conclusions may be drawn:

1. The influence of configuration of web reinforcement on beam deflections after the occurrence of the first diagonal crack was not significant for beams having openings within exterior shear spans, whereas inclined web reinforcement was the most effective form for reducing deflections of continuous deep beams having openings within interior shear spans.
2. The development of diagonal crack width was nearly independent on the configuration of web reinforcement for beams having openings within exterior shear spans. On the other hand, for beams having openings within interior shear spans, more effective control of diagonal crack width was exhibited by beams with inclined web reinforcement than beams with vertical or horizontal web reinforcement. The effect of inclined web reinforcement on

- controlling diagonal crack width was also more prominent in beams with web reinforcement above and below openings than that in beams with web reinforcement only above openings.
3. The load capacity of beams having openings within exterior shear spans was 10~15% smaller than that of the companion solid deep beams, but the shear capacity at failed shear spans of such beams dramatically decreased to 40~50% relative to that of the companion solid deep beams, irrespective of shear span-to-overall depth ratio. On the other hand, for beams having openings within interior shear spans, both the load and shear capacities sharply decreased in comparison with the companion solid deep beams.
 4. Inclined web reinforcement was the most effective type for increasing load and shear capacities of continuous deep beams with openings. In addition, the load and shear capacities of beams with web reinforcement above and below openings were higher than those beams with web reinforcement only above openings.
 5. The shear capacity of beams tested is overestimated using Kong et al's formula. However, the predictions were closer to experimental results for beams with shear span-to-overall depth ratio of 0.6 than beams with shear span-to-overall depth ratio of 1.0.

ACKNOWLEDGMENTS

This work was supported by the Korea Research Foundation Grant (KRF-2004-041-D00746). The authors wish to express their gratitude for financial support.

REFERENCES

1. Kong, F. K., and Sharp, G. R., "Shear Strength of Light Weight Reinforced Concrete Deep Beams with Web Openings," *The Structural Engineer*, V. 51, No. 8, Aug. 1973, pp. 267-275.
2. Shanmugam, N. E., and Swaddiwudhipong, S., "Strength of Fibre Reinforced Concrete Deep Beams Containing Openings," *The International Journal of Cement Composites and Lightweight Concrete*, V. 10, No. 1, Feb. 1988, pp. 53-60.
3. Yang, K. H., Eun, H. C., and Chung, H. S., "The Influence of Web Openings on the Structural Behavior of Reinforced High-Strength Concrete Deep Beams," *Engineering Structures*, Accepted, 2006.
4. Yang, K. H., Chung, H. S., and Ashour, A. F., "Influence of Inclined Web Reinforcement on the Reinforced Concrete Deep Beams with Openings," *ACI Structural Journal*, Submitted for publication, 2006.
5. Kong, F. K., Sharp, G. R., Appleton, S. C., Beaumont C. J., and Kubik, L. A., "Structural Idealization for Deep Beams with Web Openings; Further Evidence," *Magazine of Concrete Research*, V. 30, No. 103, June 1978, pp. 89-95.
6. Tan, K. H., Tong, K., and Tang, C. Y., "Consistent Strut-and-Tie modelling of Deep Beams with Web Openings," *Magazine of Concrete Research*, V. 55, No. 1, Feb. 2003, pp. 65-75.
7. Tan, K. H., Tang, C. Y., and Tong, K., "Shear Strength Predictions of Pierced Deep Beams with Inclined Web Reinforcement," *Magazine of Concrete Research*, V. 56, No. 8, Aug. 2004, pp. 443-352.
8. ACI Committee 318: *Building Code Requirements for Structural Concrete (ACI 318-05) and Commentary (ACI 318R-05)*. American Concrete Institute, 2005.

9. Canadian CSA Building Code, Design of Concrete Structures: Structures (Design)-A National Standard of Canada (CAN-A23.3-94), Clause 11.1.2, Canadian Standards Association. Toronto, 1994.
10. CEB-FIP MC 90, Design of Concrete Structures. CEB-FIP Model Code 1990, Thomas Telford, London, 1993.
11. CIRIA, The Design of Deep Beams in Reinforced Concrete (CIRIA 2). Ove Arup & Partners and CIRIA, London, 1997.
12. Ashour, A. F., "Tests of Reinforced Concrete Continuous Deep Beams," ACI Structural Journal, V. 94, No. 1, Jan.-Feb. 1997, pp. 3-12.
13. Rogowsky, D. M., and MacGregor, J. G., and Ong, S. Y., "Tests of Reinforced Concrete Deep Beams," ACI Journal, V. 83, No. 4, July-Aug. 1986, pp. 614-623.
14. Yang, K. H. Chung, H. S., and Ashour, A. F., "Influence of Shear Reinforcement on Reinforced Concrete Continuous Deep Beams," ACI Structural Journal, submitted for publication, 2006.
15. Ashour, A. F., and Rishi, G., "Tests of Reinforced Concrete Continuous Deep Beams with Web Openings," ACI Structural Journal, V. 97, No. 3, May-June 2000, pp. 418-426.

TABLES AND FIGURES

List of Tables:

Table 1 – Details of Test Specimens

Table 2 – Details of test results and predictions

List of Figures:

Fig. 1 – Specimen details and arrangement of web reinforcement around openings.

Fig. 2 – Test setup.

Fig. 3 – Typical crack patterns and failure of beams tested.

Fig. 4 – Mid-span deflection against total load of beams having $a/h=0.6$.

Fig. 5 – Support reaction against total load for beams without web reinforcement.

Fig. 6 – $(R_E)_{Exp.}/(R_E)_{FE}$ according to configuration of web reinforcement.

Fig. 7 – Diagonal crack width against total load of beams having $a/h=0.6$.

Fig. 8 – Strain of web reinforcement against total load for beams having $a/h=0.6$.

Fig. 9 – Effect of web reinforcement configuration on λ_n .

Fig. 10 – Effect of web reinforcement configuration on η_n .

Fig. 11 - Structural idealization of simple deep beams with web openings by Kong et al.

Fig. 12 – Comparison of predicted and measured shear capacities at failed shear span with openings.

Table 1–Details of Test Specimens

Specimen	f'_c (MPa)	a/h	L (mm)	Openings			Web reinforcement around openings*					
				Location	Width (mm)	Depth (mm)	V	H	I	Position		
6N	60.7	0.6	720	None			-	-	-	-		
6ENN	50.5			Exterior shear spans	180 (=0.5a)	120 (=0.2h)	-	-	-	-		
6EVU							3Φ 10	-	-	Above		
6EHU							-	3Φ 10	-			
6EIU							-	-	3Φ 10			
6INN				60.7	Interior shear spans	180 (=0.5a)	120 (=0.2h)	-	-	-	-	
6IVU								3Φ 10	-	-	Above	
6IHU								-	3Φ 10	-		
6IIU								-	-	3Φ 10		
6IVB	3Φ 10							-	-	Above		
6IHB	-							3Φ 10	-	+		
6IIB	-			-	3Φ 10	Below						
10N	48.1			1.0	1200	None			-	-	-	-
10ENN						Exterior shear spans	360 (=0.5a)	120 (=0.2h)	-	-	-	-
10EVU		3Φ 10	-						-	Above		
10EHU		-	3Φ 10						-			
10EIU		-	-						3Φ 10			
10INN		60.7	Interior shear spans			360 (=0.5a)	120 (=0.2h)	-	-	-	-	
10IVU								3Φ 10	-	-	Above	
10IHU								-	3Φ 10	-		
10IIU								-	-	3Φ 10		
10IVB								3Φ 10	-	-	Above	
10IHB								-	3Φ 10	-	+	
10IIB		50.5	-			-	3Φ 10	Below				

* V, H, and I stand for vertical, horizontal, and inclined web reinforcement, respectively. Above and Below also means the upper chord above openings and the lower chord below openings, respectively.

Table 2-Details of test results and predictions

Specimen	Load (P_{cr}) and shear force (V_{cr}) at the first diagonal crack, (kN)								Failure load (P_n) and ultimate shear force (V_n) at failed interior shear span, (kN)				Failure mode	$(V_n)_{Pro.}^{\#}$ kN	$\frac{(V_n)_{Pro.}}{(V_n)_{Exp.}}$
	W-span				E-span				P_n	λ_n $= \frac{P_n / 2}{b_w h \sqrt{f'_c}}$	V_n	η_n $= \frac{V_n}{b_w h \sqrt{f'_c}}$			
	Interior		Exterior		Interior		Exterior								
	P_{cr}	V_{cr}	P_{cr}	V_{cr}	P_{cr}	V_{cr}	P_{cr}	V_{cr}							
6N	1250	369	2260	574	1090	328	2260	566	2860	1.912	828	1.107	A	1114	1.346
6ENN	916	314	861	136	1009	356	816	120	2310	1.693	790 (365*)	1.158 (0.535)	B	412	1.129
6EVU	1040	368	853	133	1039	357	873	139	2324	1.703	787 (376*)	1.153 (0.550)	B	431	1.148
6EHU	833	282	788	127	1166	399	843	128	2432	1.782	803 (413*)	1.177 (0.605)	B	435	1.052
6EIU	1000	348	545	94	1019	364	701	104	2462	1.804	779 (452*)	1.142 (0.662)	B	444	0.982
6INN	529	146	970	239	559	158	1014	242	1459	1.069	341	0.500	A	412	1.208
6IVU	531	148	1000	233	579	160	785	182	1830	1.341	438	0.642	A	431	0.984
6IHU	549	154	1039	276	525	153	1012	234	1723	1.263	399	0.585	A	435	1.089
6IIU	466	143	1039	223	697	211	1020	215	1998	1.464	516	0.756	A	444	0.860
6IVB	508	140	1093	261	587	163	1128	269	2114	1.549	537	0.787	A	498	0.928
6IHB	640	163	2067	550	640	170	2067	541	2053	1.372	509	0.681	A	534	1.049
6IIB	380	111	2600	815	540	148	2460	695	2437	1.629	681	0.910	A	629	0.923

Table 2 (continued)-Details of test results and predictions

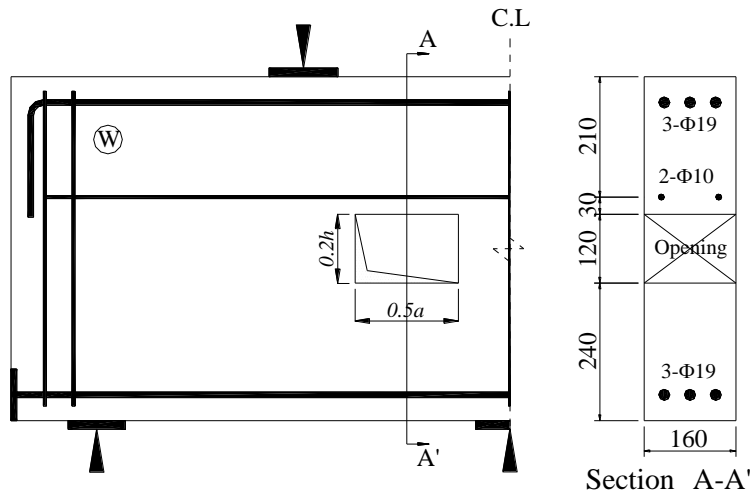
Specimen	Load (P_{cr}) and shear force (V_{cr}) at the first diagonal crack, (kN)								Failure load (P_n) and ultimate shear force (V_n) at failure span, (kN)				Failure mode	$(V_n)_{Pro.}$ # kN	$\frac{(V_n)_{Pro.}}{(V_n)_{Exp.}}$
	W-span				E-span				P_n	λ_n $= \frac{P_n / 2}{b_w h \sqrt{f'_c}}$	V_n	η_n $= \frac{V_n}{b_w h \sqrt{f'_c}}$			
	Interior		Exterior		Interior		Exterior								
	P_{cr}	V_{cr}	P_{cr}	V_{cr}	P_{cr}	V_{cr}	P_{cr}	V_{cr}							
10N	600	207	-	-	600	203	-	-	1208	0.907	388	0.583	A	821	2.115
10ENN	755	272	366	50	569	208	366	49	1039	0.780	368 (151*)	0.552 (0.227)	B	230	1.521
10EVU	931	332	310	49	931	329	735	110	1089	0.817	374 (170*)	0.561 (0.255)	B	264	1.555
10EHU	767	281	471	63	925	335	423	56	1153	0.865	396 (180*)	0.594 (0.270)	B	241	1.337
10EIU	696	251	475	70	948	346	428	65	1214	0.911	413 (194*)	0.620 (0.291)	B	257	1.323
10INN	195	62	-	-	215	69	-	-	831	0.555	182	0.243	A	249	1.367
10IVU	300	78	-	-	300	81	-	-	1024	0.684	239	0.320	A	283	1.186
10IHU	348	108	-	-	227	75	-	-	946	0.693	211	0.309	A	244	1.159
10IIU	230	73	-	-	220	72	-	-	1083	0.724	279	0.373	A	276	0.988
10IVB	359	115	-	-	343	110	925	185	1057	0.775	310	0.454	A	374	1.207
10IHB	304	94	765	181	385	118	639	142	1009	0.739	244	0.358	A	281	1.151
10IIB	185	66	852	181	301	98	840	176	1311	0.961	382	0.560	A	414	1.084
Mean															1.15
Standard deviation															0.18

Note) Mean and standard deviation were calculated for all beams, excluding the continuous solid deep beams

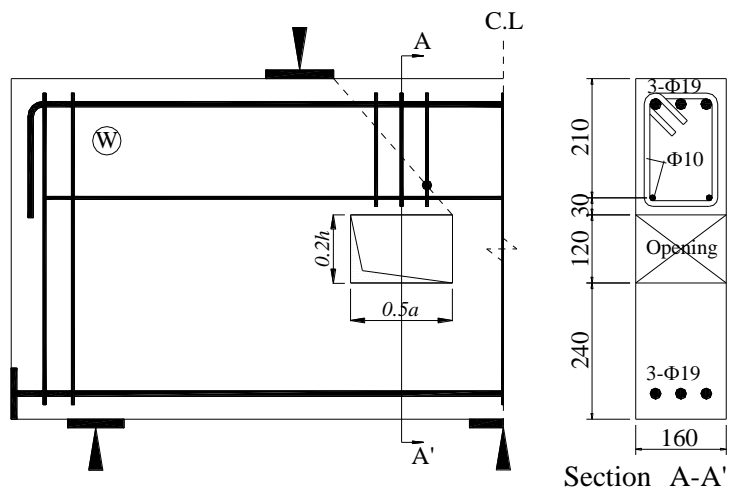
- indicates that diagonal cracks did not occur at exterior shear spans.

* Ultimate shear force at failed exterior shear span.

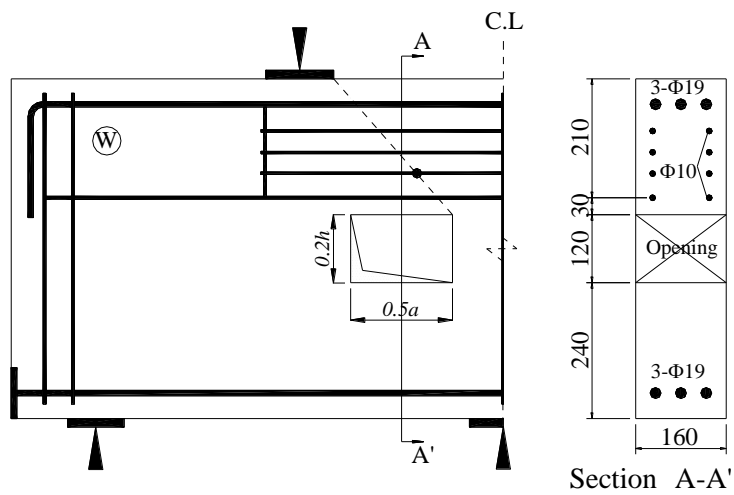
Predictions obtained from Kong et al's formula⁵ based on test results of simple deep beams with openings.



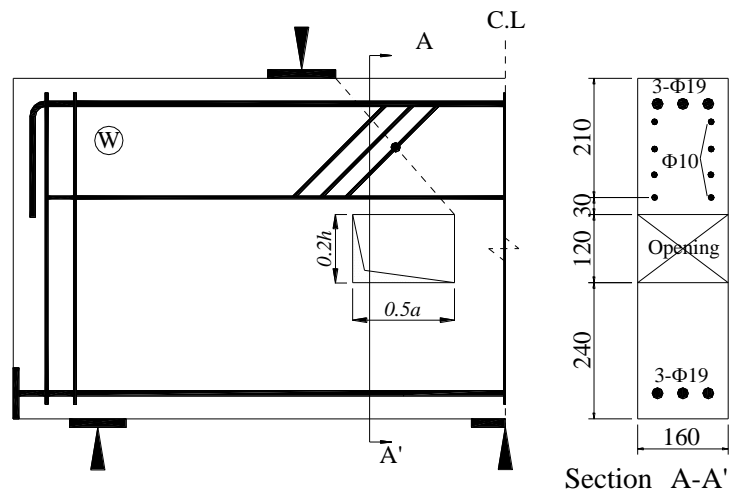
(a) Beams without web reinforcement around openings



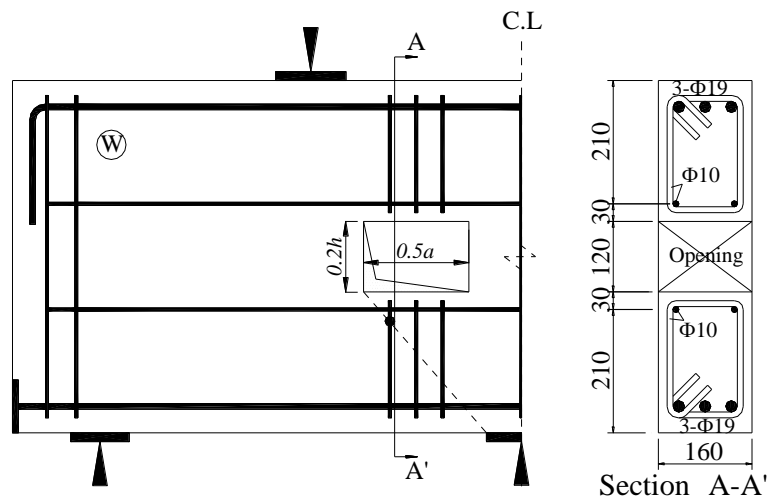
(b) Beams with vertical reinforcement above openings (U-type)



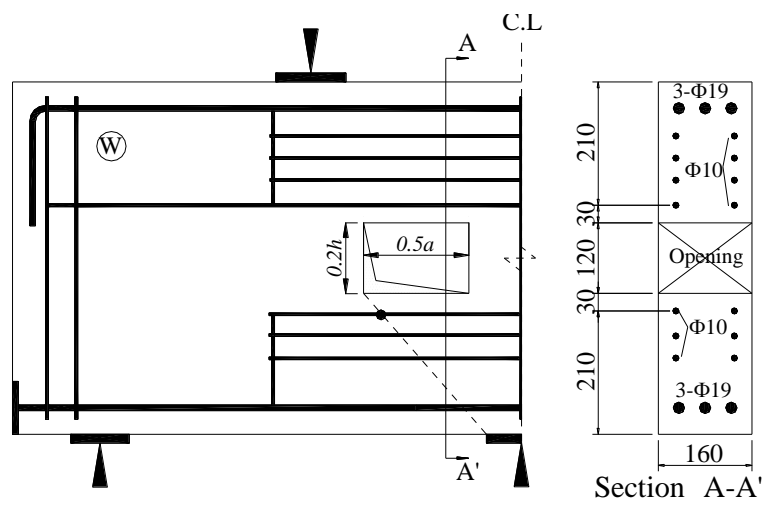
(c) Beams with horizontal reinforcement above openings (U-type)



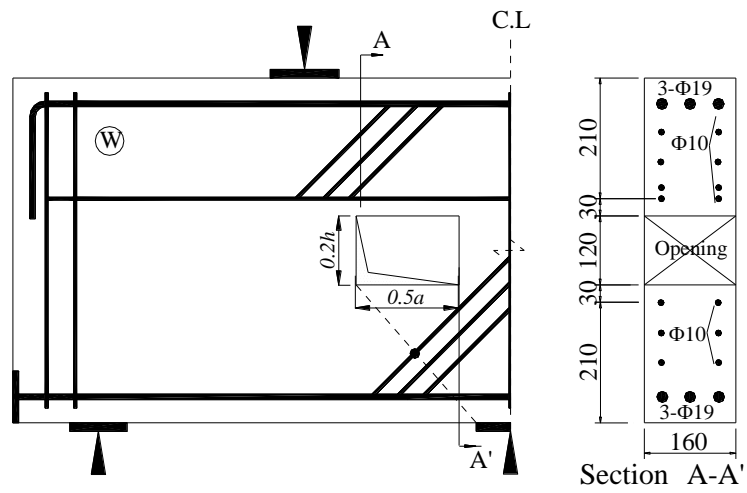
(d) Beams with inclined reinforcement above openings (U-type)



(e) Beams with vertical reinforcement in above and below openings (B-type)



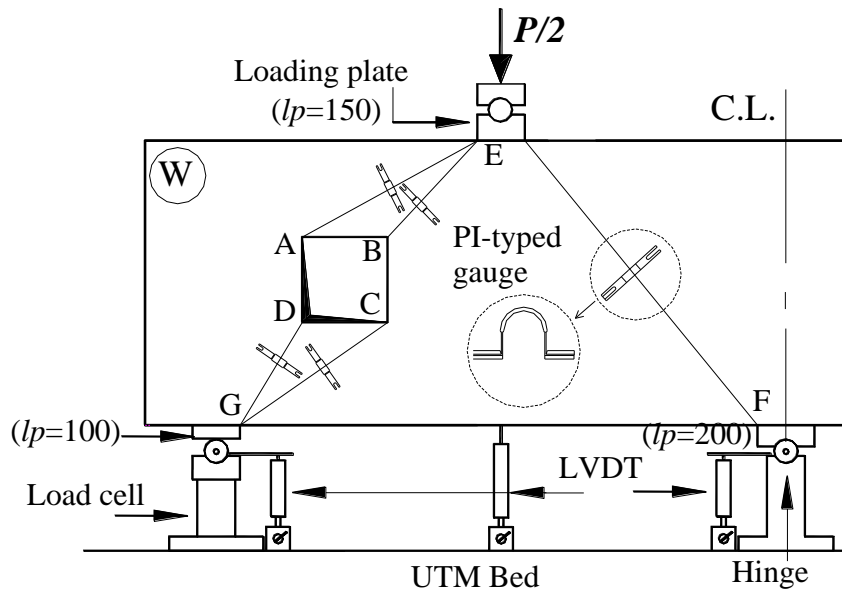
(f) Beams with horizontal reinforcement in upper and lower chords (B-type)



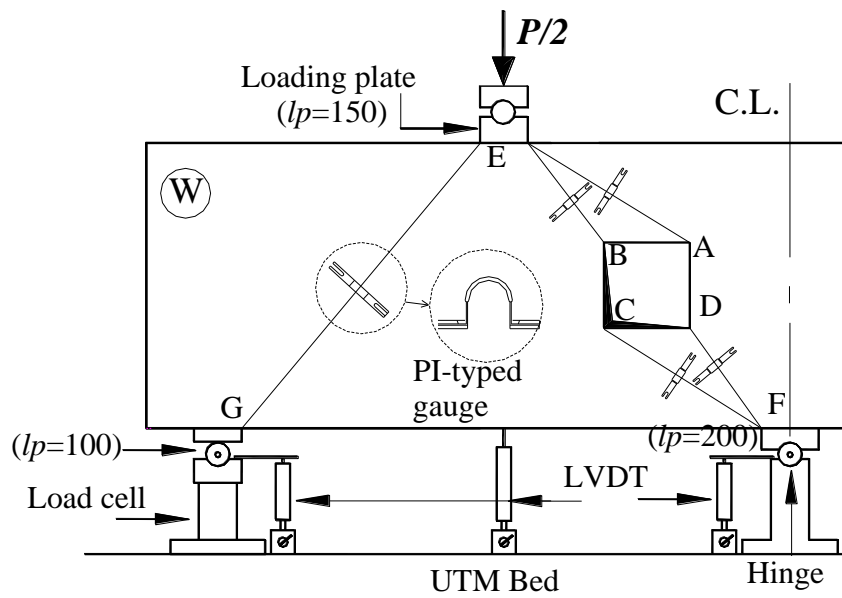
(g) Beams with inclined reinforcement above and below openings (B-type)

Fig. 1-Specimen details and arrangement of web reinforcement around openings.

**Note: ‘●’ indicates positions of ERS gauges.
All dimensions are in mm.**

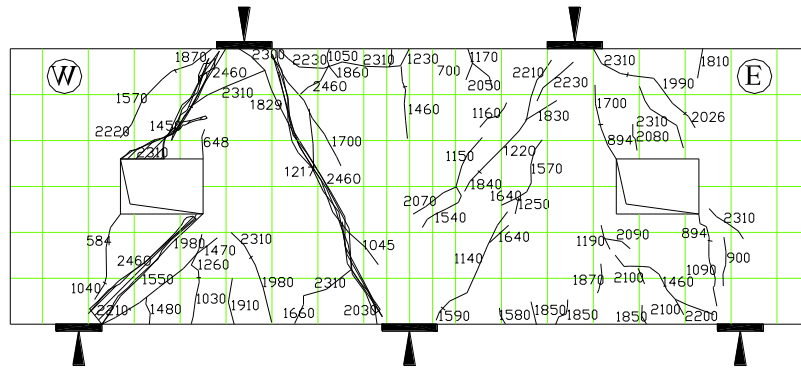


(a) Beams having web openings within exterior shear spans

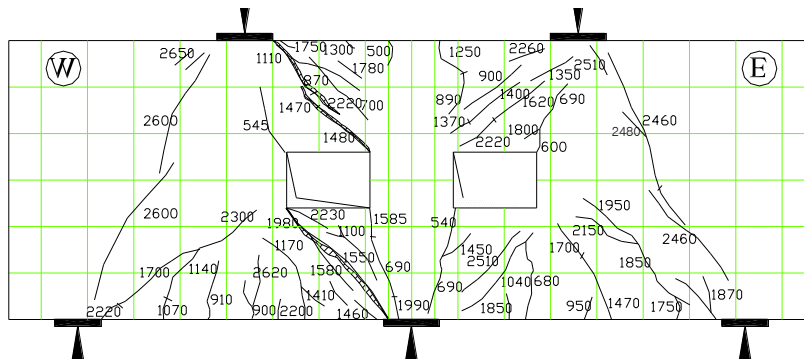


(b) Beams having web openings within interior shear spans

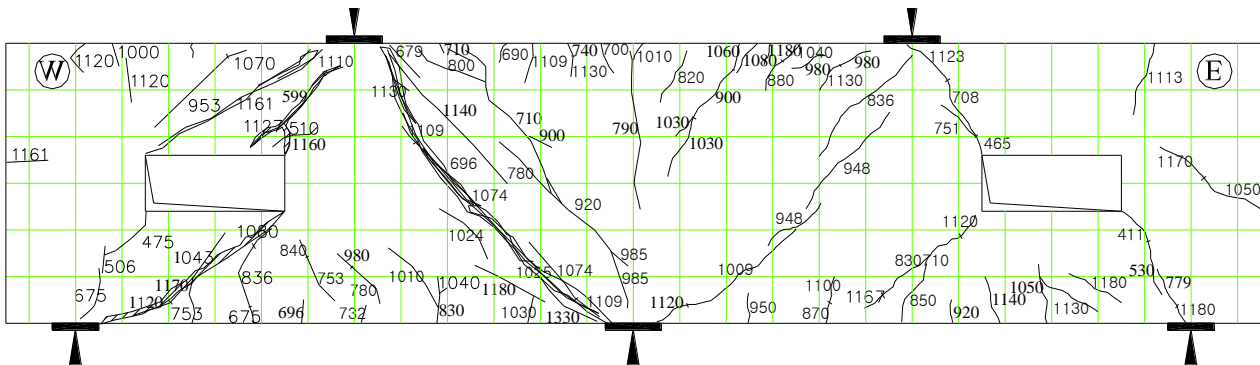
Fig. 2-Test setup (all dimensions are in mm).



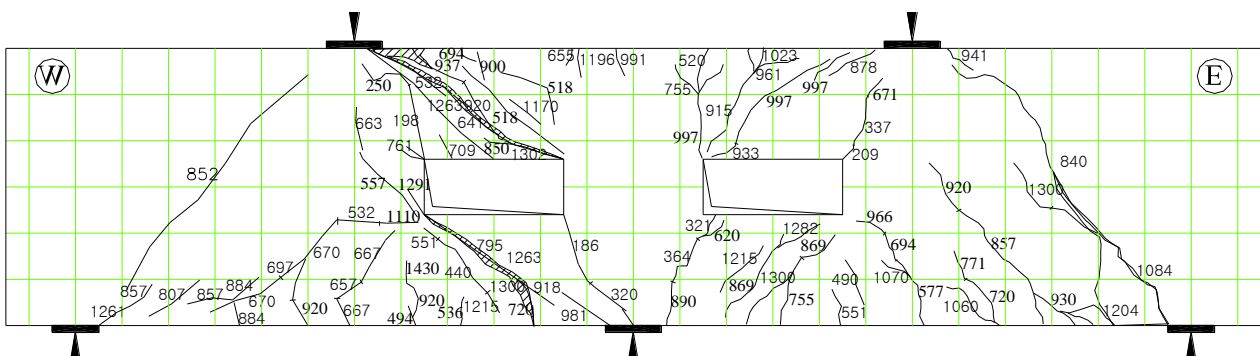
(a) 6EIU



(b) 6IIB

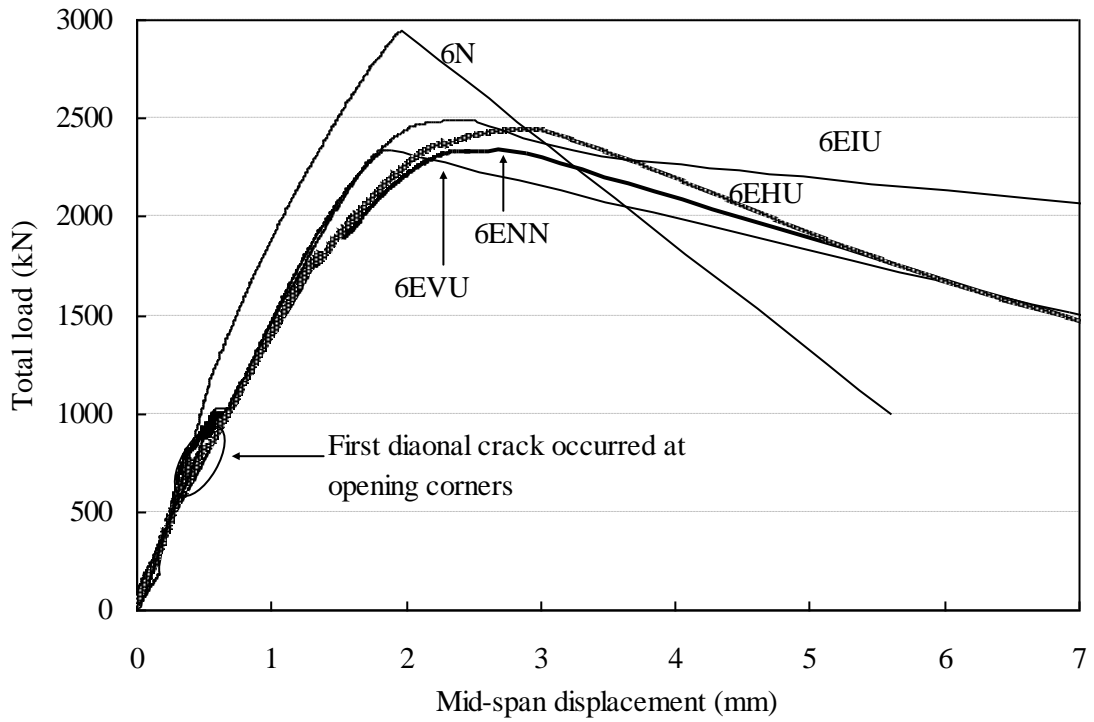


(c) 10EIU

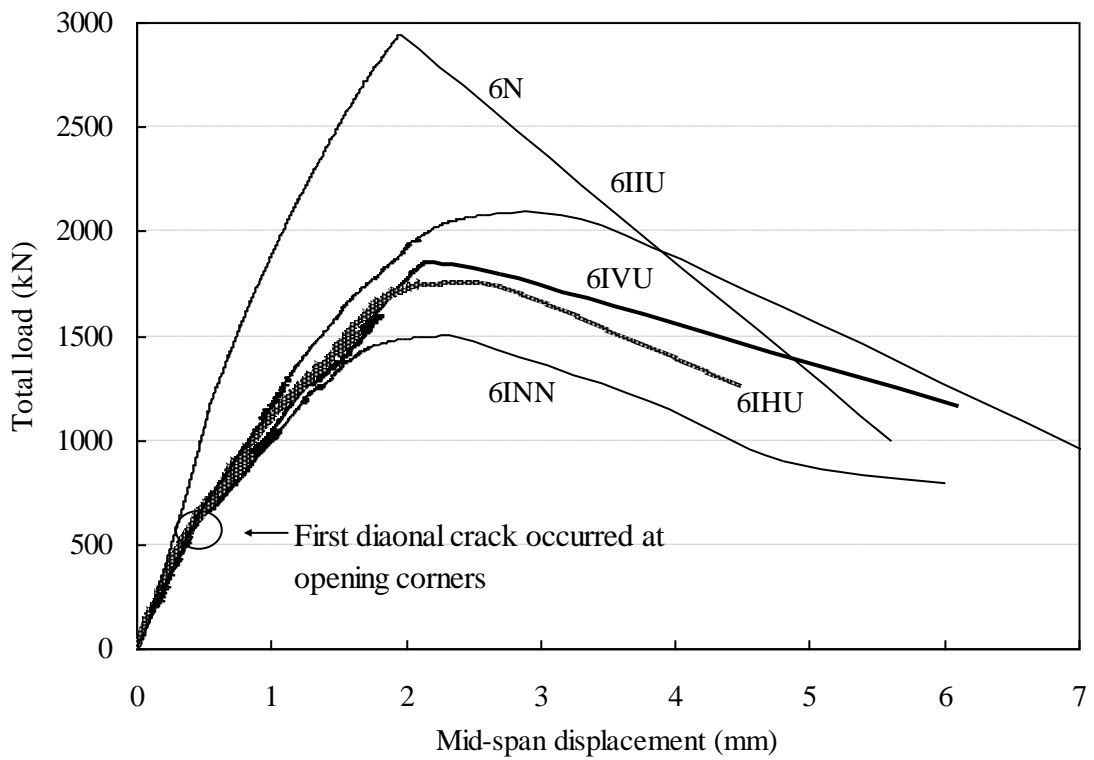


(d) 10IIB

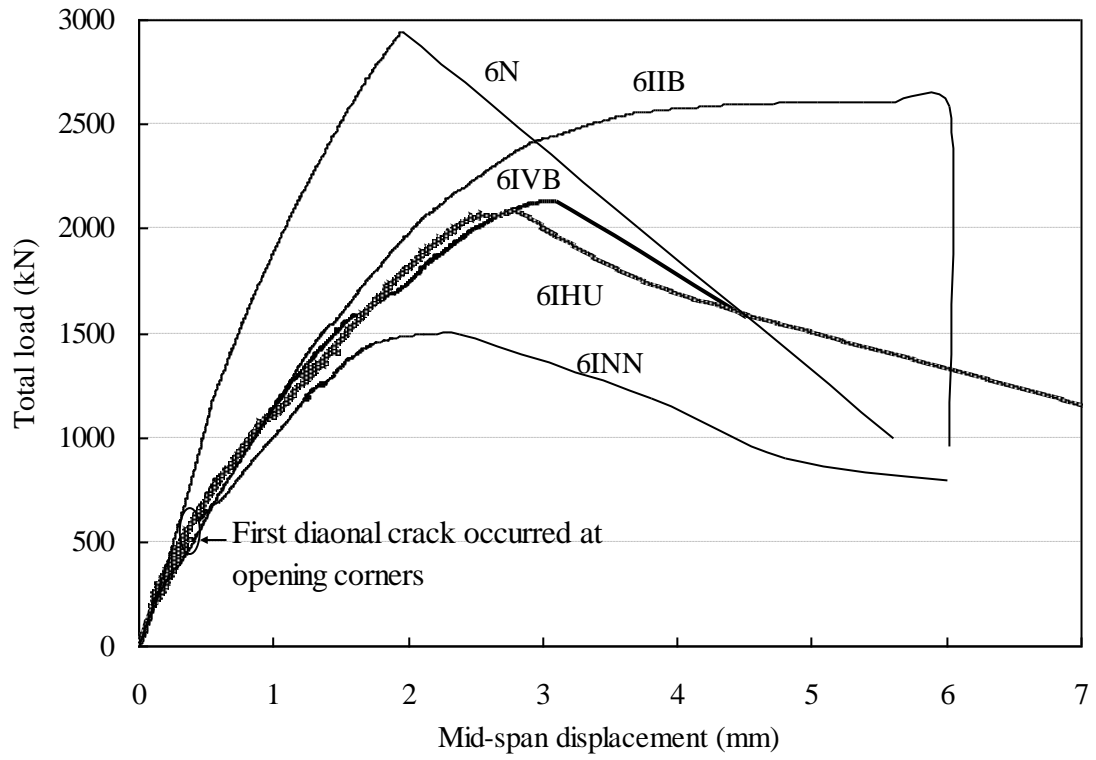
**Fig. 3– Typical crack patterns and failure modes of beams tested
(Numbers indicate the total load in kN at which cracks occurred.)**



(a) Beams having openings within exterior shear spans (U-type)

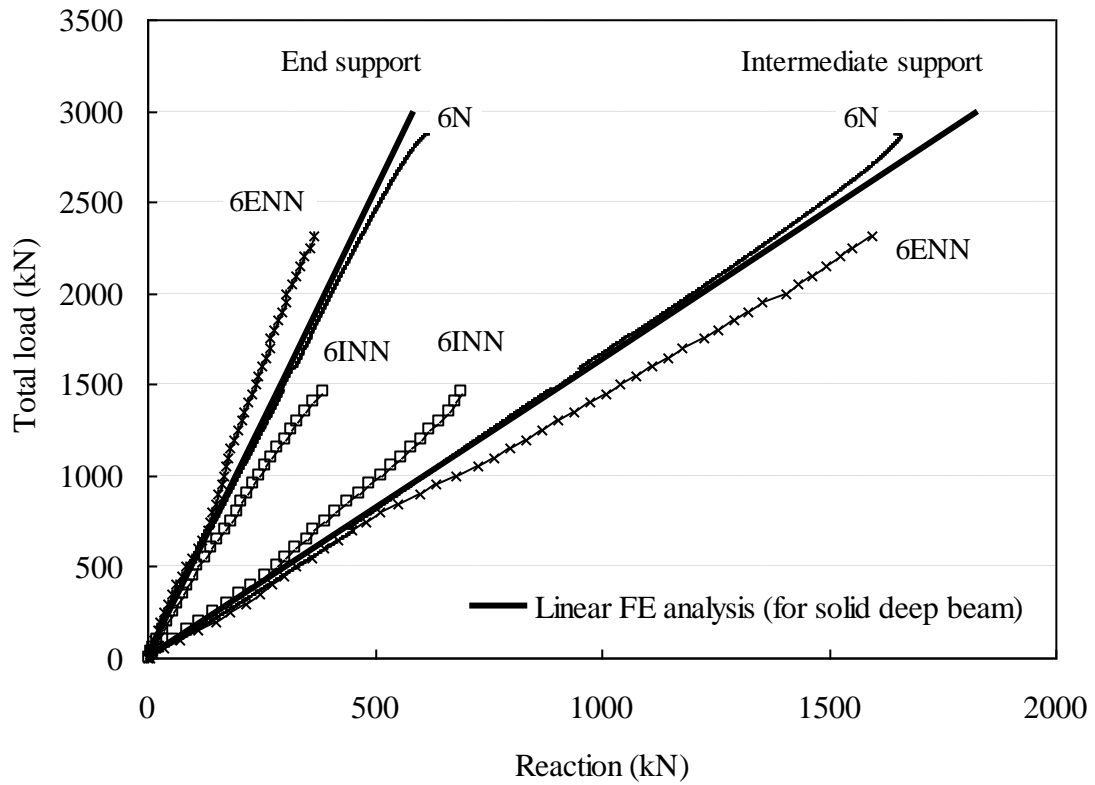


(b) Beams having openings within interior shear spans (U-type)

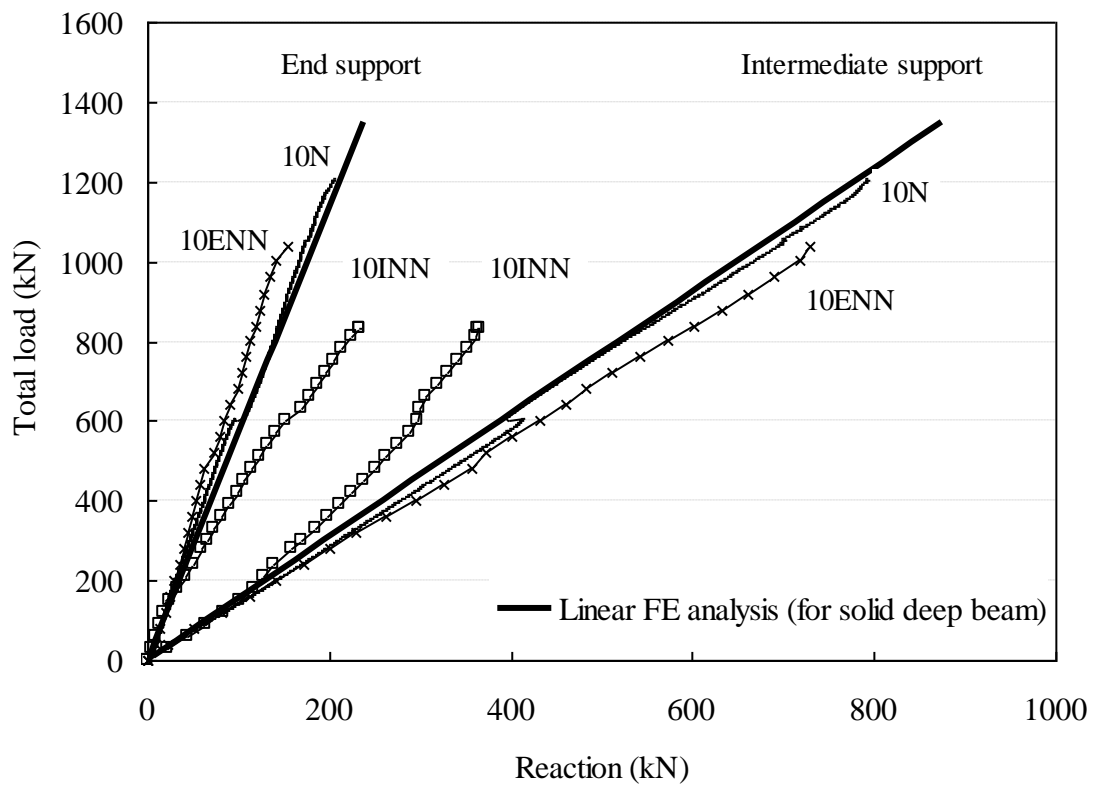


(c) Beams having openings within interior shear spans (B-type)

Fig. 4—Mid-span deflection against total load of beams having $a/h=0.6$.

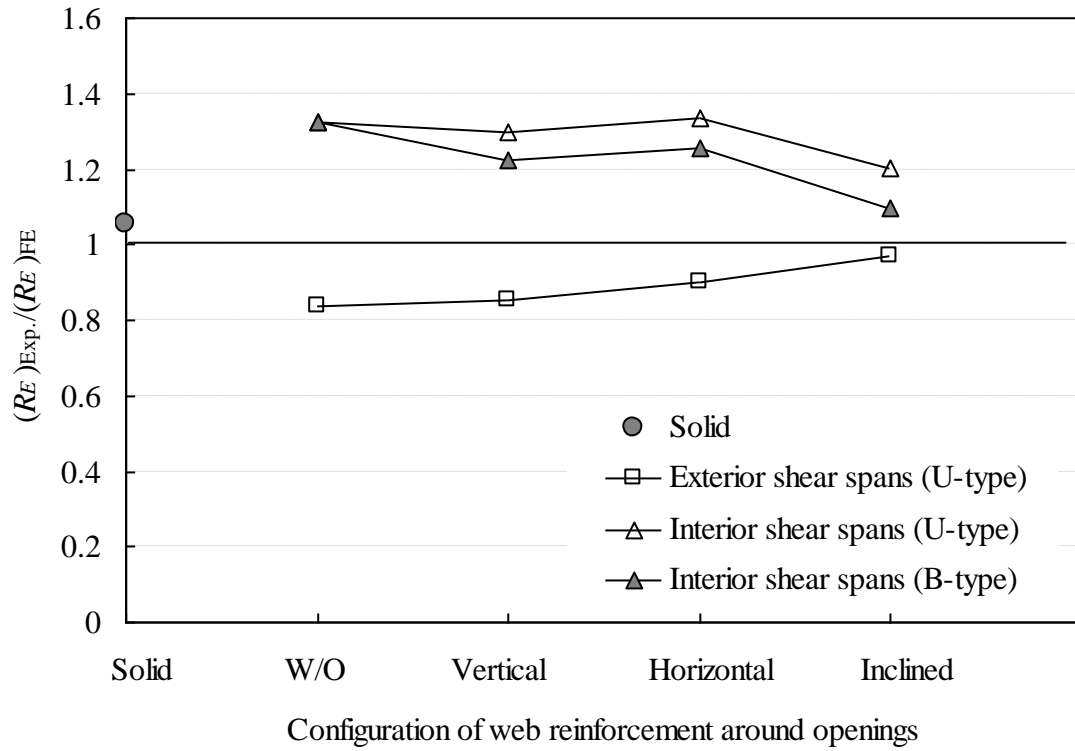


(a) $a/h = 0.6$

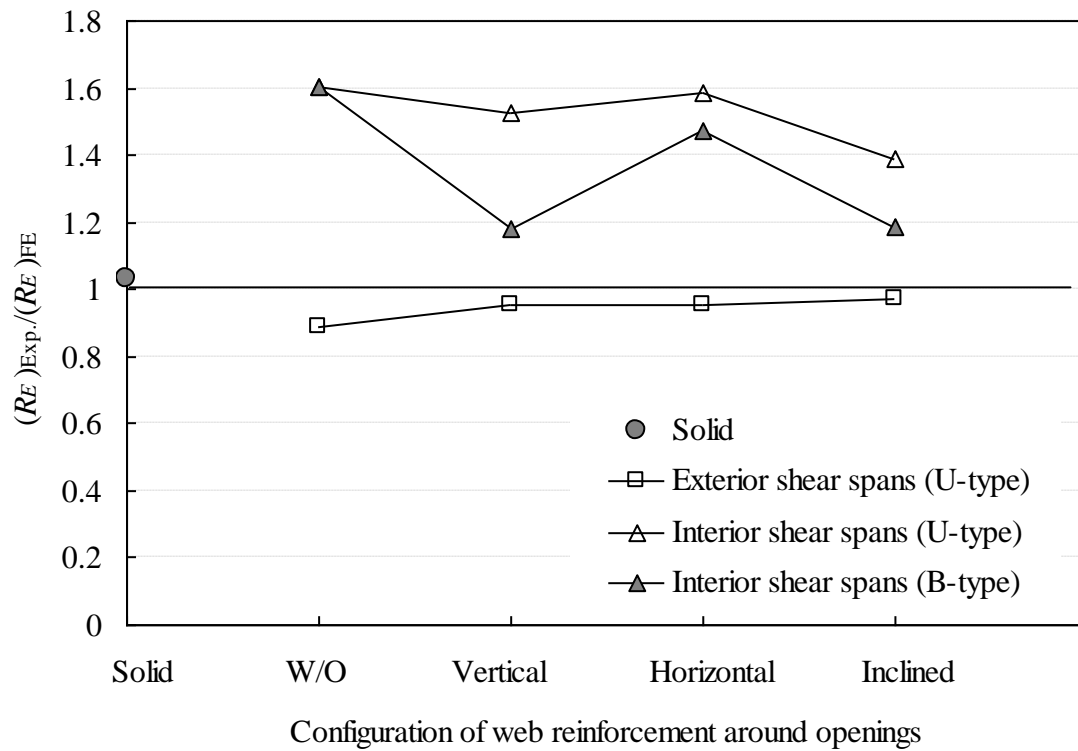


(b) $a/h = 1.0$

Fig. 5—Support reaction against total load for beams without web reinforcement.

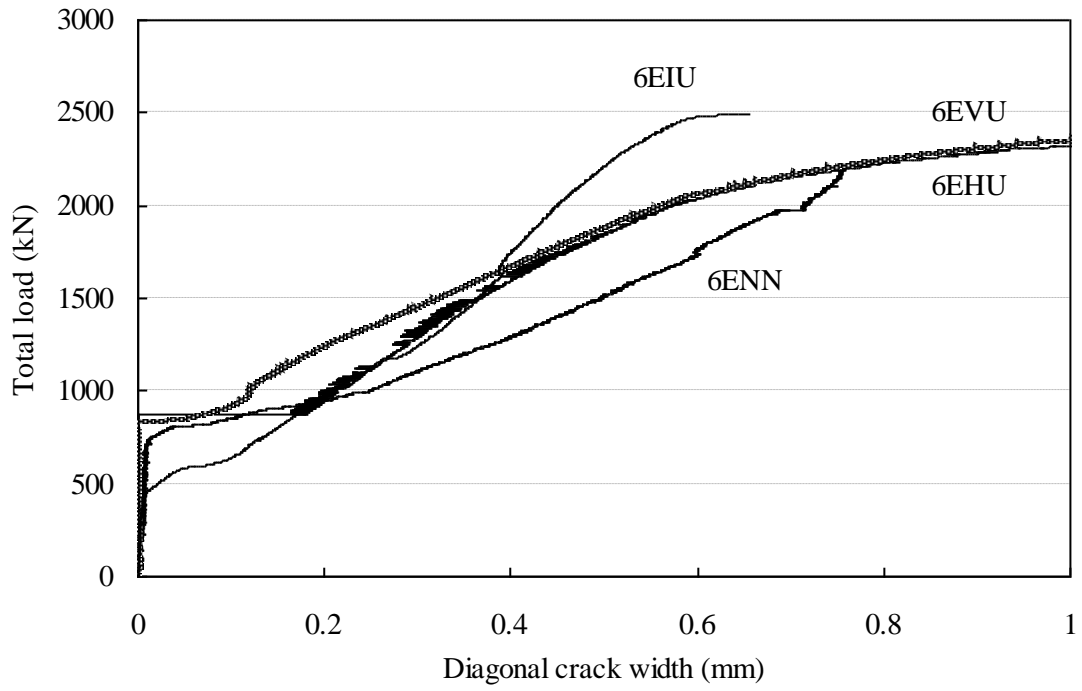


(a) $a/h = 0.6$

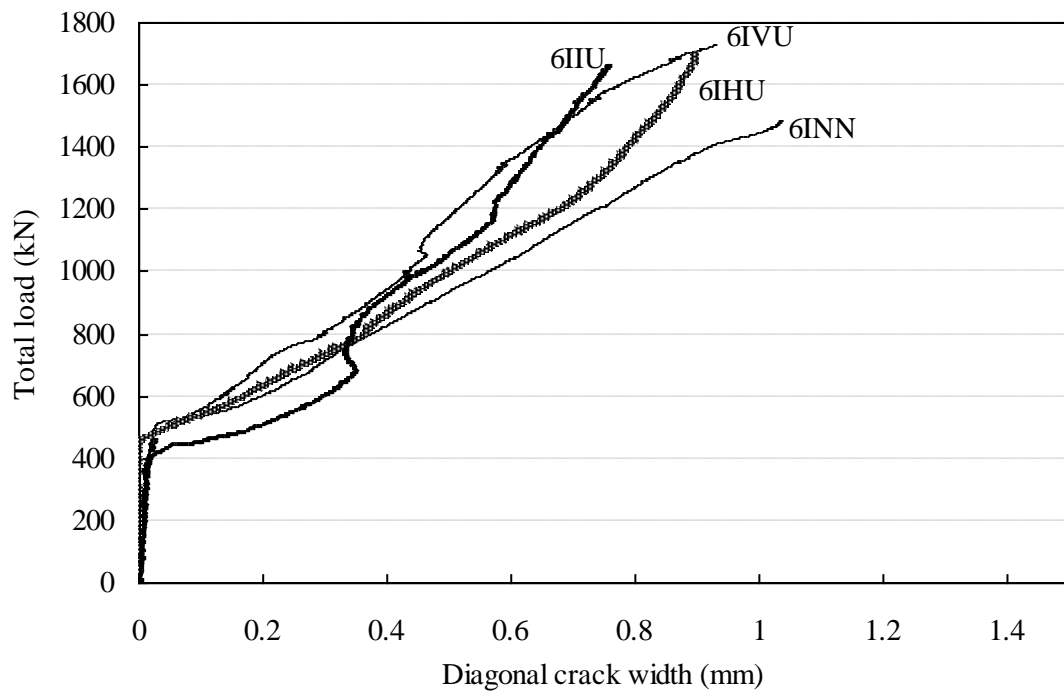


(b) $a/h = 1.0$

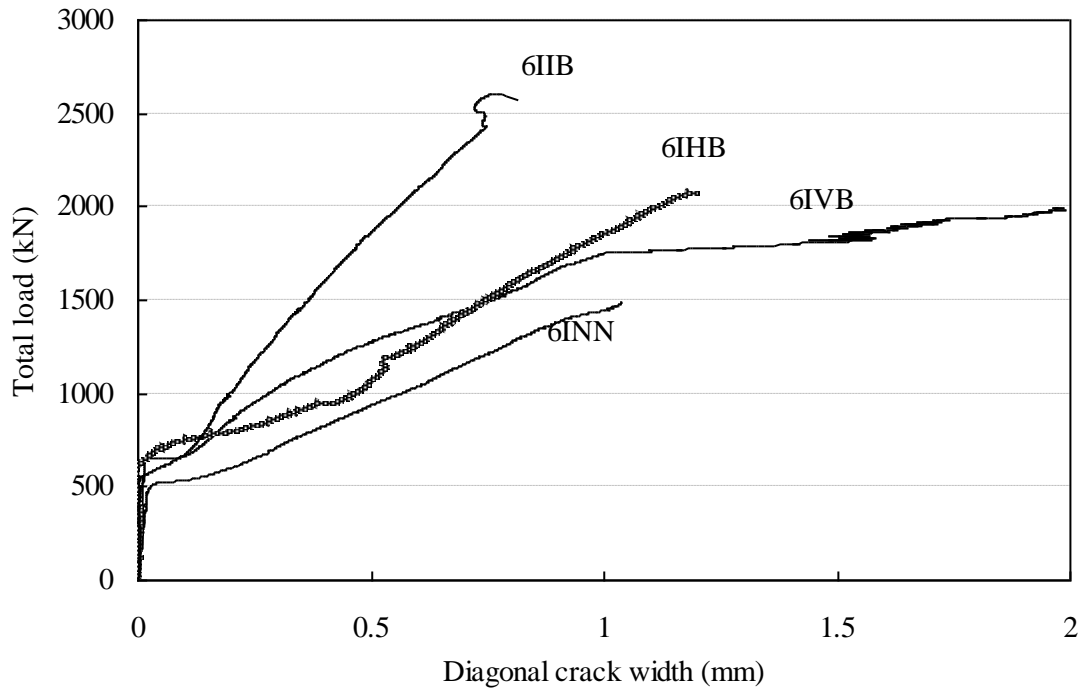
Fig. 6— $(R_E)_{Exp.}/(R_E)_{FE}$ according to configuration of web reinforcement around openings.



(a) Beams having openings within exterior shear spans (U-type)



(b) Beams having openings within interior shear spans (U-type)



(c) Beams having openings within interior shear spans (B-type)

Fig. 7–Diagonal crack width against total load of beams having $a/h=0.6$.

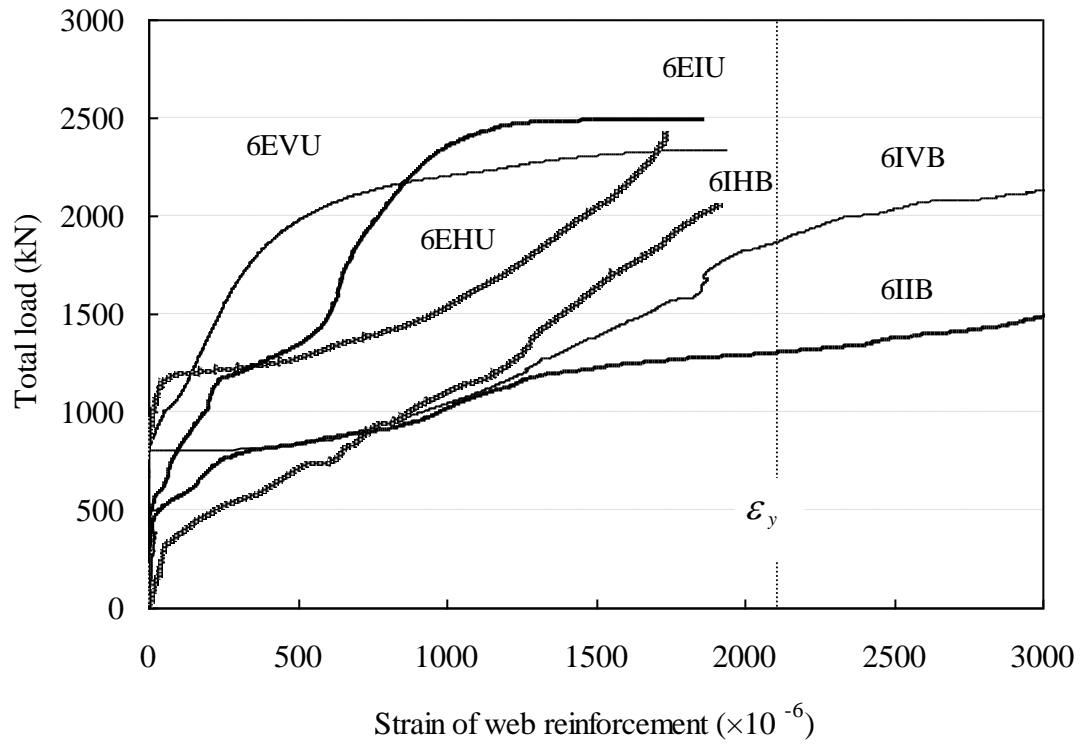


Fig. 8—Strain of web reinforcement against total load for beams having $a/h=0.6$.

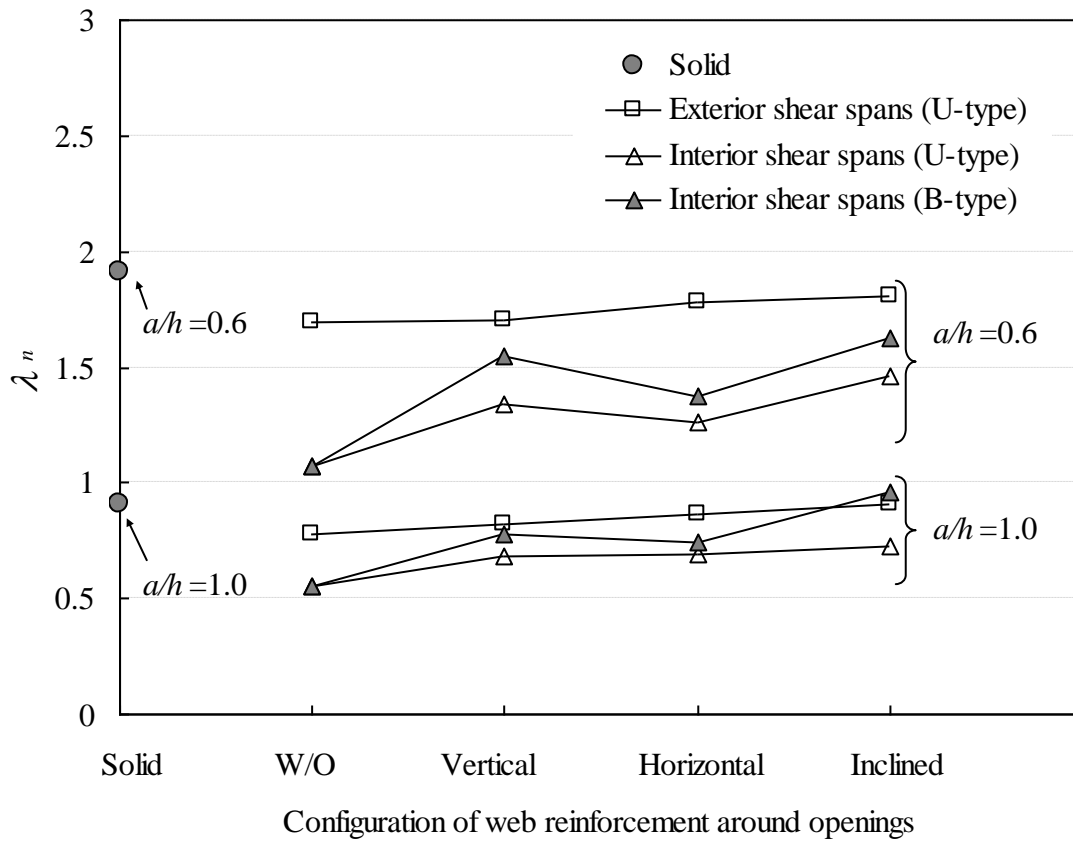


Fig. 9—Effect of web reinforcement configuration on λ_n .

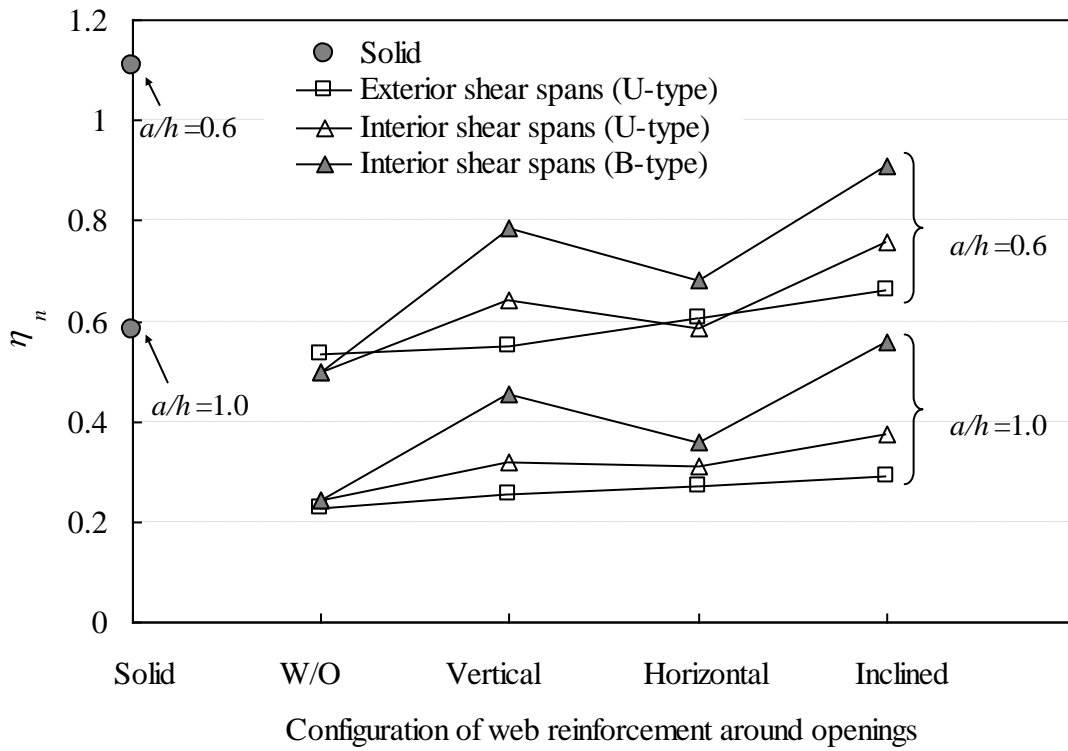


Fig. 10—Effect of web reinforcement configuration on η_n .

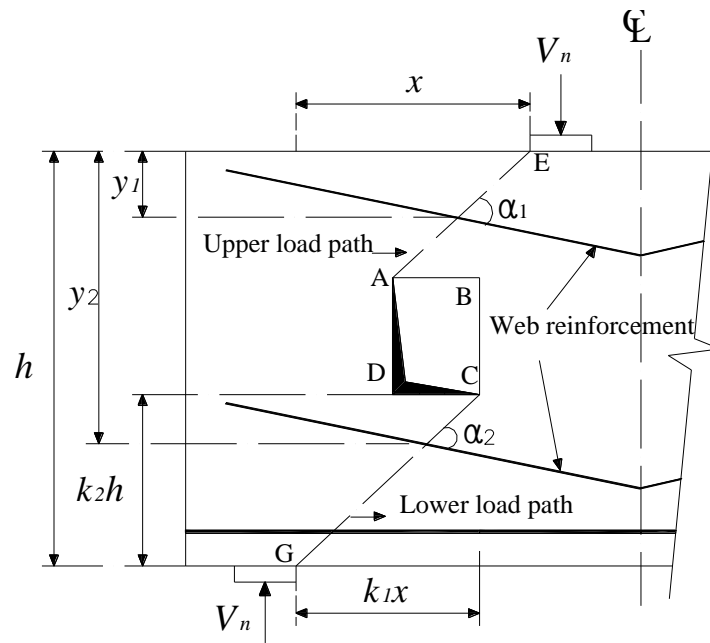
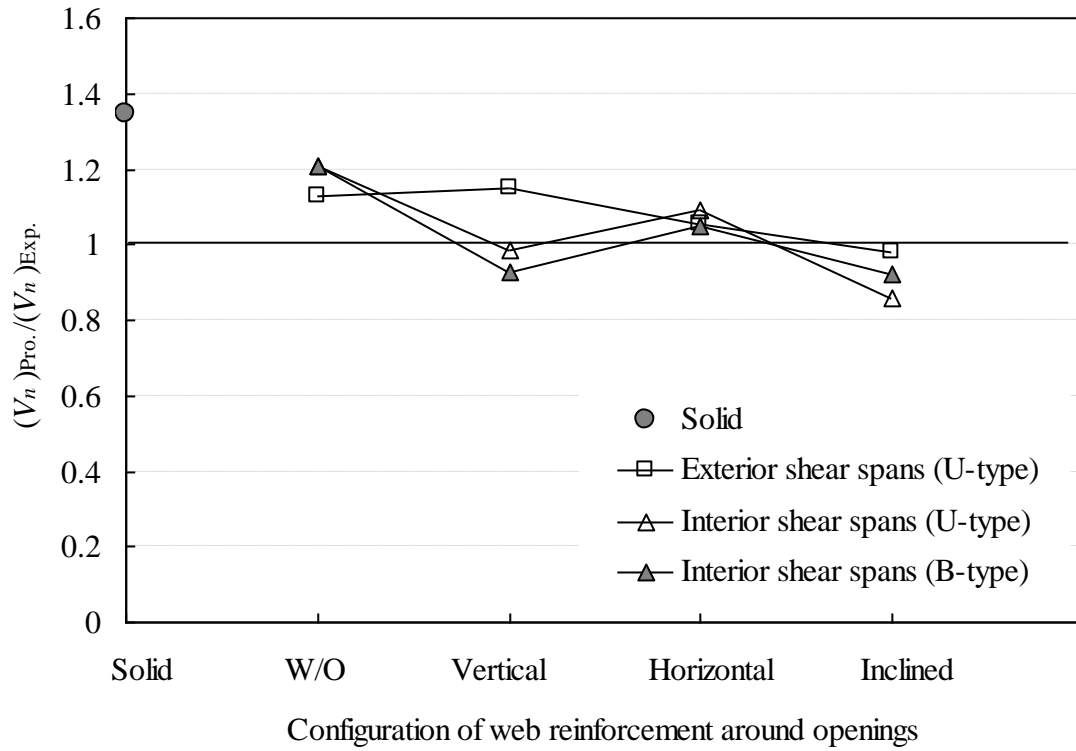
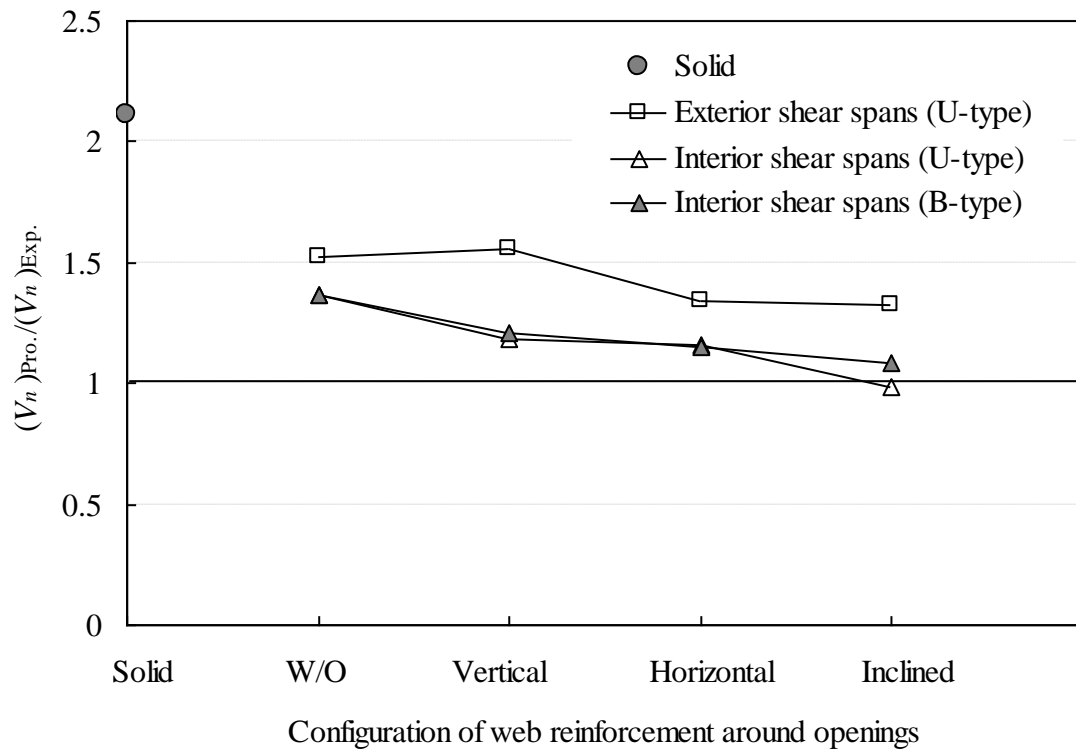


Fig. 11–Structural idealization of simple deep beams with web openings by Kong et al⁵.



(a) $a/h = 0.6$



(b) $a/h = 1.0$

Fig. 12–Comparison of predicted and measured shear capacities at failed span with openings.